Phys. Status Solidi C **11**, No. 11–12, 1593–1596 (2014) / **DOI** 10.1002/pssc.201400053

physica status solidi c
www.pss-c.com
current topics in solid state physics

Electrically detected magnetic resonance study on defects in Si pn-junctions created by proton implantation

Gernot Gruber[*,1,2], Stefan Kirnstoetter[2,3], Peter Hadley[,2], Markus Koch[4], Thomas Aichinger[3], Holger Schulze[3], and Werner Schustereder[3]**

[1] KAI GmbH, Europastrasse 8, 9500 Villach, Austria
[2] Institute of Solid State Physics, Graz University of Technology, Petersgasse 16, 8010 Graz, Austria
[3] Infineon Technologies Austria, Siemensstrasse 2, 9500 Villach, Austria
[4] Institute of Experimental Physics, Graz University of Technology, Petersgasse 16, 8010 Graz, Austria

Received 29 April 2014, revised 9 May 2014, accepted 12 May 2014
Published online 13 August 2014

Keywords EDMR, defects, silicon, hydrogen, implantation, pn-junction

* Corresponding author: e-mail gernot.gruber@k-ai.at, Phone: +43 316 873-8960, Fax: +43 316 873-108461
** e-mail p.hadley@tugraz.at, Phone: +43 316 873-8967, Fax: +43 316 873-108461

The present study focuses on electrically detected magnetic resonance (EDMR) investigations of proton implanted silicon. The samples were prepared on n-type silicon wafers highly doped diffused boron (B) p-region, forming a pn-junction. A large additional n-type doping was introduced by proton (H^+) implantation. We compare samples with implantation doses up to 10^{15} H^+/cm^{-2} and investigate the effects of anneals at 350 °C. We observe different types of defects in the differently prepared samples. One doublet with 118.5 G HF splitting and a *g*-value of 2.0095(4) is only observed in the samples implanted with the highest dose and is assigned to hydrogen. The structure of the other observed defects remains unidentified and can only tentatively be assigned to hydrogen. More extensive measurements would have to be performed to get a better picture.

1 Introduction Due to their light weight protons (H^+) can be implanted deep into silicon (Si) and are used for various applications in the power semiconductor device manufacturing. Depending on the implantation dose, H^+ implantations are used to introduce recombination centers to locally adjust the charge carrier lifetime [1], to form hydrogen related thermal donor profiles (HTDs) [2] or to cleave thin wafers due to very high damage concentrations [3]. In this study we are mainly interested in the microscopic structures of HTD complexes formed due to implantations in the dose range from 10^{14} to 10^{15} H^+/cm^2 and subsequent anneals at 350 °C [2, 4]. It has been shown in various studies that the concentration and type of thermal donor generated strongly depends on the annealing temperature and annealing time [5]. However, the concrete structure/nature of these defects is still under debate [6].

Electrically detected magnetic resonance (EDMR) is an experimental technique where the change of a current in a fully processed semiconductor device is used as a means to obtain the electron spin resonance (ESR) spectrum of electrically active defects in the device. Point defects in semiconductors often contain unpaired electrons. ESR is the measurement of transitions between the Zeeman levels of the unpaired electrons in a magnetic field. The transitions are induced by a microwave field. Resonance is obtained when the microwave photons match the energy difference between the Zeeman levels. The resonance condition is

$$h\nu = g\mu_B B\,, \tag{1}$$

with Planck's constant h, microwave frequency ν, Landé factor g, Bohr magneton μ_B, and magnetic field B [7]. The parameter g and its angular dependence contain structural information about the observed defects. Additional information can be gained from the hyperfine (HF) structure of the spectra. HF lines are observed due to the presence of nearby paramagnetic nuclei, i.e. atoms with nuclear magnetic spin. The local magnetic field close to such a paramagnetic nucleus is slightly altered due to the magnetic field induced by the nuclear spin. Therefore, the resonance

is observed at a shifted magnetic field for electrons located at paramagnetic nuclei. For protons with nuclear spin $I = 1/2$ two configurations of the nucleus are possible and therefore two lines are observed. ESR is conventionally measured in the absorbed microwave power which limits the sensitivity. The detection limit is 10^{10} unpaired electrons. As electrical measurements are very sensitive, EDMR allows for the detection of much smaller total numbers of defects [8]. A common way to measure EDMR is spin dependent recombination (SDR). A forward bias applied to a pn-junction results in a current of which a fraction is the trap-assisted recombination of carriers in the depletion region. This part of the current may change when the unpaired electrons of point defects in the depletion region become resonant [8, 9]. This allows for the measurement of the ESR spectra of the defects in the depletion region by measuring the change in the device current. Trap assisted recombination is most efficient for defects close to midgap which is why only this energy region can be probed [10].

2 Experimental The goal was to obtain a high dose of H^+ induced defects within the depletion region of the pn-junction. However, while a higher dose causes a higher defect concentration and therefore a potentially higher signal one has to consider that it also narrows the depletion region and therefore decreases the volume that can be probed. Furthermore, if the doping of the p-region does not exceed the doping of the n-region, most of the depletion region would be on the rather undamaged p-side of the junction. Therefore, care in the sample manufacturing had to be taken so that p > n while n was as high as possible. The substrate was a 725 µm thick float zone n-Si wafer with a phosphorous (P) concentration of 6.8×10^{13} cm^{-3}. In order to obtain a high doping concentration in the p-region the substrate was implanted with boron (B) at 170 keV and a dose of 1×10^{14} cm^{-2}. The B was then diffused at 1100 °C for 400 min resulting in a 5 µm wide p-region, with a doping concentration of $p \approx 10^{15} - 3 \times 10^{17}$ cm^{-3}. Afterwards the samples were implanted with H^+ at different energies and doses in order to obtain an n-type peak close to the high B doped region. The best results were obtained using an implantation energy of 450 keV and implantation doses of 10^{14} cm^{-2} (sample 1) and 10^{15} cm^{-2} (sample 2). A third sample with no H^+ implantation (sample 3) was prepared as a reference. All samples were measured before (labeled N) and after an annealing at 350 °C for one hour (labeled A). Figure 1 shows the doping profiles of all samples obtained by spreading resistance profiling (SRP) measurements with a cross section angle of 0.847 degrees. The upper graph shows the sample 1, the middle graph sample 2 and the lower graph sample 3. All doping profiles reveal a pn-junction (indicated by vertical lines) where the doping of the p-side is higher than on the n-side, particularly in the region close to the junction. This means that the depletion region and thus the probed volume is mainly on the n-side and allows for an EDMR measurement of the defects caused by the H^+ implantation. In samples 1 and 2 the large introduction of donors in a depth of about $x = 4$-5 µm results in a change from p-type to n-type and an associated shift of the pn-junction depth. This shift is larger for sample 2 which received a 10 times higher dose than sample 1. Comparing the annealed samples with the not annealed ones reveals changes in the doping profiles for samples 1 and 2 while in samples 3 no changes can be observed. For this reason sample 3N was no longer considered as no differences to sample 3A were expected.

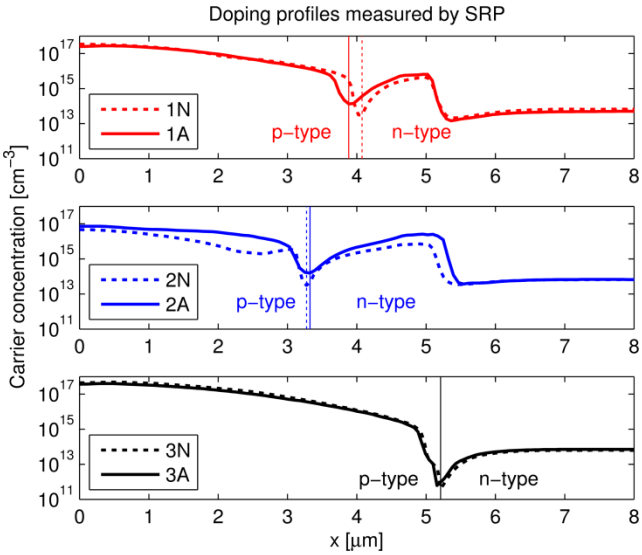

Figure 1 Doping profiles measured by spreading resistance profiling with a cross section angle of 0.847 degrees.

For the EDMR measurements the samples need to be forward biased under conditions that allow for efficient carrier recombination. This means the ideality-factor η from the diode equation

$$I \propto \exp(qV / \eta k_B T) \quad (1)$$

should be close to 2 [11]. In order to find the best biasing conditions the *IV*-characteristics were recorded, which are shown in Fig. 2. The characteristics of the samples A show a similar behavior while the samples N clearly differ. From these curves the best biasing voltages for the EDMR measurements were determined to be 160 mV for sample 2N, and 190 mV for the other samples. The EDMR measurements were performed with an X-band ESR spectrometer with a microwave frequency of $f_{mw} = 9.4$ GHz and a microwave power of 27 dBm. The samples were put in a TE_{103} cavity with a quality factor of $Q \approx 3500$. All measurements were performed at room temperature. The magnetic field was modulated at $B_1 = 2$G with a frequency of $f_1 = 780$ Hz in order to apply lock-in-amplification. The magnetic field was calibrated using a 2,2-diphenyl-1-picrylhydrazyl (DPPH) standard with $g = 2.0036(2)$ [12].

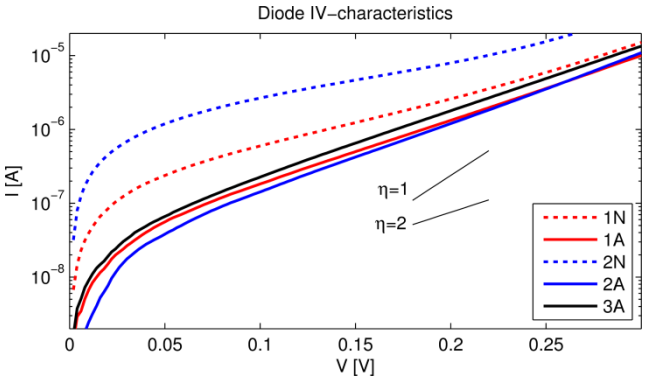

Figure 2 *IV*-characteristics of the pn-junctions.

3 Results and discussion The EDMR measurements of all three samples with *B* parallel to the crystalline [100] direction are shown in Fig. 3. Sample 3A shows a pair of peaks which can be assigned to intrinsic defects in the material. As the doping on the p-side of this sample is two orders of magnitude higher than on the n-side, the depletion region must extend mainly into the n-side. This side, despite the tail of the diffused B, mostly contains the defects of the raw semiconductor substrate. The peaks are labeled I1 and I2 and are due to two separate defects as their relative intensities determined from Gaussian fits are 35 % and 65 % respectively. These defects are most likely vacancies or vacancy-oxygen complexes.

All the other samples clearly show different spectra. Most of the spectra still contain a pair of peaks close to the center. However, the peaks appear at different magnetic field and with different relative intensities. Recalling the doping profiles from Fig. 1 there is one major difference between sample 3 and the rest. Samples 1 and 2 have an n-doping about 2 orders of magnitude higher than sample 3. Therefore the depletion width in sample 3 is much larger and the probed volume much higher. For this reason it is plausible that the (small) concentration of intrinsic defects is simply not observed in samples 1 and 2 or just overshadowed by the higher concentration of defects due to the H^+ implant. It is therefore not likely that these defects are the same as I1 and I2, which is why they are labeled H1 and H2.

The annealed samples generally show a much higher signal than the not annealed ones. As observed in Figs. 1 and 2 the not annealed samples show very different doping profiles and *IV*-characteristics, making them less comparable. It can be concluded that these samples are unfavorable for the study of the H+ induced defects. Whether the reason is simply the shape and uniformity of the doping profiles or rather the anneal itself cannot be concluded with certainty. However, it has been shown in prior studies that an annealing above 350 °C plays an important role in the donor formation process in silicon [5].

Due to the higher implantation dose sample 2 shows a richer spectrum than sample 1. The intensity of H1 and H2 is clearly higher. More importantly, a doublet (labeled D) with a hyperfine splitting of 118.5 G and a *g*-value of 2.0095(4) is observed only in sample 2, both before and after the anneal. A doublet can only be produced by a spin ½ atom, which suggests a defect related to H. Sample 2 received a 10 times higher H^+ dose than sample 1 which is probably the reason why the doublet cannot be observed in sample 1. We conclude that there are at least two different types of defects present in sample 2A. One related to H causing the small D on the sides and one or more causing H1 and H2.

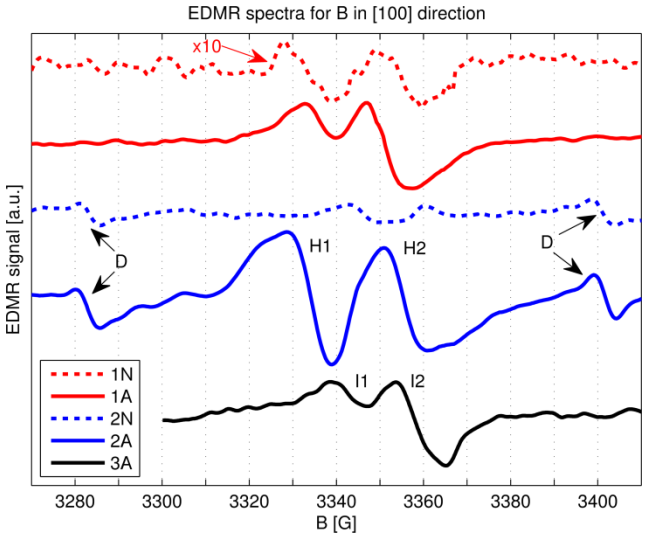

Figure 3 EDMR spectra of all samples with B parallel to the [100] direction. The spectra are vertically offset for better comparison. The spectrum of sample 1N has be enlarged by a factor of 10 due to its small intensity.

One problem in understanding the nature of H1 and H2 comes from the fact that the pn-junction, and therefore the region probed by EDMR, in sample 2A is in a region with a B content much higher than in sample 3A. This higher B content may interfere with the measurement as it may introduce another type of defect or simply change the recombination processes. It remains unclear how comparable samples 2A and 3A really are.

In order to get a better understanding of H1 and H2 and their relation to I1 and I2, samples 2A and 3A were measured at angles ranging from 0 °-90 ° between *B* and the [100] axis. The whole tilt series is shown in Fig. 4. It becomes clear from this that I1 and I2 are most likely not related to H1 and H2 as the angular behavior is very different. Despite an overlapping of the right peak of sample C with a peak of sample B at 0 ° and 90 °, there is no good match in between, which suggests that the samples show different types of defects. Particularly for angles around 50 ° no good match is observed. What also becomes clear from this tilt series is the fact that H1 and H2 are in fact more than two peaks. It appears as if H1 and H2 were actually two or more doublets that change their position and hyper-

fine splitting with the angle. H1 and H2 could be due to a H related defect with similar behavior to the AA9 or AA2 defects reported by Gorelkinskii et al. [13-15]. This means that one defect doublet in its different possible orientations in the crystal produces all overlapping peaks observed in the tilt series. If this observation is correct it would mean that not only D, but all defects appearing in sample 2A are H related. As the resolution of the shown spectra is not high enough to obtain clearly resolved peaks for all angles, more extensive and time consuming studies will have to be performed.

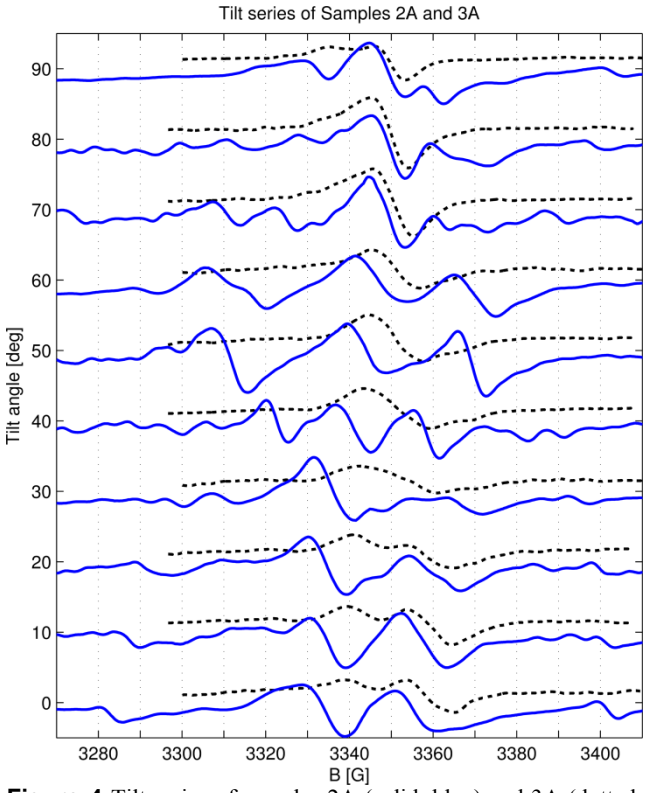

Figure 4 Tilt series of samples 2A (solid, blue) and 3A (dotted, black). 0 deg corresponds to the [100] direction.

4 Conclusion We report on the EDMR measurements of defects created in a Si pn-junction by proton implantation. A clear change in the EDMR response is observed in comparison to a not implanted reference sample indicating that the implantation not only results in an n-type doping, but also in the introduction of recombination centers. The not implanted sample contains two types of defects, most likely intrinsic defects of the semiconductor material. The implanted samples show different patterns dependent on the annealing and the implantation dose. A clear identification of the defects causing the large EDMR response was not achieved, yet they are most likely hydrogen related. In samples with a very high implantation dose a clearly hydrogen related doublet appears.

Acknowledgements We thank Wolfgang E. Ernst (Institute of Experimental Physics, TU Graz) for enabling and supporting the project, Gregor Pobegen (KAI GmbH) for fruitful discussions, and Guenter Grampp (Institute of Physical and Theoretical Chemistry, TU Graz) for lending us the ESR equipment. This work was jointly funded by the Austrian Research Promotion Agency (FFG, Project No. 831163) and the Carinthian Economic Promotion Fund (KWF, contract KWF-1521|22741|34186).

References

[1] P. Hazdra, K. Brand, J. Rubeš, and J. Vobecký, Microelectron. J. **32**(5), 449-456 (2001).
[2] Y. Zohta, Y. Ohmura, and M. Kanazawa, Jpn. J. Appl. Phys. **10**(4), 532-533 (1991).
[3] S. Romani and J. H. Evans, Nucl. Instrum. Methods Phys. Res. B **44**(3), 313-317 (1990).
[4] S. Kirnstoetter, M. Faccinelli, W. Schustereder, L. G. Laven, H.-J. Schulze, and P. Hadley, AIP Conf. Proc. **1583**, 51 (2014).
[5] C. S. Fuller, J. A. Ditzenberger, N. B. Hannay, and E. Buehler, Phys. Rev. **96**, 833 (1955).
[6] E. Simoen, Y.L. Huang, Y. Ma, J. Lauwart, P. Clauws, J.M. Rafí, A. Ulyashin, and C. Claeys, J. Electrochem. Soc. **156**(6), H434(2009).
[7] J.A. Weill, J.R. Bolton, and J.E. Wertz, Electron Paramagnetic Resonance (John Wiley & Sons, New York, 1994), pp. 21.
[8] D.J. Lepine, Phys. Rev. B **6**(2), 436(1972).
[9] D. Kaplan, I. Solomon, and N.F. Mott, J. Physique – Lettres **39**, 51 (1978
[10] M.A. Jupina and P.M. Lenahan, IEEE Trans. Nucl. Sci. **36**, 1800 (2009).
[11] S.M. Sze and K.K. Ng, Physics of Semiconductor Devices (John Wiley & Sons, Hoboken, 2007), p. 98.
[12] J. Krzystek, A. Sienkiewicz, L. Pardi, and L.C. Brunel, J. Magn. Res. **125**(1), 207 (1997).
[13] Y.V. Gorelkinskii and N.N. Nevinnyi, Phys. Lett. **99**A(2,3), 117 (1983).
[14] Y.V. Gorelkinskii and N.N. Nevinnyi, Physica B **170**, 155 (1991).
[15] Y.V. Gorelkinskii and N.N. Nevinnyi, Mater. Sci. Eng. B **36**, 133 (1996).

